ISSN 8755-6839

SCIENCE OF **TSUNAMI HAZARDS**

Journal of Tsunami Society International

Volume 40 **Number 1** **2021**

EVALUATION OF SEISMIC AND TSUNAMI RESISTANCE OF POTENTIAL SHELTERS FOR VERTICAL EVACUATION IN CASE OF A TSUNAMI IMPACT IN BAHIA DE CARÁQUEZ, CENTRAL COAST OF ECUADOR

Pablo Ezequiel Suárez-Acosta[1], Cristian David Cañamar-Tipan[1], Darlin Alexis Ñato-Criollo[1], Juan Daniel Vera-Zambrano[1], Kevinn Luis Galarza-Vega[1], Paola Michelle Guevara-Álvarez[1], Cintya Natali Fajardo-Cartuche[1], Kimberlyn Karen Herrera-Garcés[1], Carlos Vicente Ochoa-Campoverde[1], Jhandry Santiago Torres-Orellana[1], Willington Rentería[2], Kervin Chunga[3], Oswaldo Padilla[1], Izar Sinde-González[1], Débora Simón-Baile[1] and Theofilos Toulkeridis[1,4]*

[1]Universidad de las Fuerzas Armadas ESPE, Sangolquí, Ecuador
[2]University of Southern California, Los Angeles, USA
[3]Universidad Técnica de Manabí, Portoviejo, Ecuador
[4]Universidad de Especialidades Turisticas, Quito, Ecuador
*Corresponding author: ttoulkeridis@espe.edu.ec

ABSTRACT

Ecuador has been the target of many tsunamis in its past documented history. Therefore, we performed a detailed assessment of the seismic and tsunami resistance of existing buildings, which may serve as temporary potential shelters in Bahía de Caráquez,in the coast of Ecuador. Prior to this evaluation we used the extensively validated tsunami modelling tool, which allowed to yield tsunami run up and tsunami amplitude based on a modelized 8Mw event, near the studied area. Furthermore, we calculated and elaborated evacuation times and routes based on the assumption of a potential tsunami impact, with a veriety of GIS tools. Based on the short time of reaction for the vulnerable population within the potential flooded area, we opted to suggest a nearby solution with a vertical evacuation in buildings along the coastal line. In order to evaluate the potential of such 26 buildings, we used the Modified Italian Methodology in order to calculate the seismic vulnerability index (SVI) and later also determine the tsunami vulnerability index (TVI).

The results indicate that only one of the 26 assessed buildings fall within acceptable values below 30 for both, SVI and TVI. As all buildings are of private property, both entrance and stairs remains limited for the general public, hence, new regulations should improve access during a tsunami emergency within an evacuation plan as well as an installed early alert system.

Keywords: *Vertical evacuation, physical structural vulnerability, tsunami resistance, early alert system, Ecuador*

1. INTRODUCTION

Tsunamis are a destructive force of nature, especially where human settlements have been constructed in their course of flow (Pararas-Carayannis, 1977; Pararas-Carayannis, 2002; Pararas-Carayannis, 2003; Pararas-Carayannis, 2006; Pheng et al., 2006; Pararas-Carayannis, 2010; Mikami et al., 2012; Rodriguez et al., 2016; Toulkeridis et al., 2017a; Rodriguez et al., 2017). Such phenomenon occurs relatively frequently and worldwide but predominantly in coastal areas, of which the major appearance is related to the Pacific Ring of Fire, which includes the coasts of Ecuador in northwestern South America (Pararas-Carayannis, 2012; Chunga and Toulkeridis, 2014; Pararas-Carayannis, 2017; Toulkeridis et al., 2017b). Like many other countries, which are situated in this geodynamic setting, Ecuador has suffered the impact of a variety of tsunamis within the recorded history and beyond as indicated by historic documents, eye witness reports and paleo-tsunami deposits (Chunga and Toulkeridis, 2014; Ioualalen et al., 2014; Chunga et al., 2017; 2018; Toulkeridis et al., 2018; Toulkeridis et al., 2019). Hereby, the past and recent destructive events demonstrated the high vulnerability of the infrastructure and population as well as the low degree of preparation of the corresponding authorities and the public (Celorio-Saltos et al., 2018; Matheus-Medina et al., 2018; Edler et al., 2020; Martinez and Toulkeridis, 2020). Due to the developments of the societies, it has been inevitably to construct human settlements and their associated needs in areas of a high degree of vulnerability towards the impact zones of tsunamis, without considering recurrent natural processes which may turn to become disasters (Alcántara-Ayala, 2002; Papathoma & Dominey-Howes, 2003; Frankenberg et al., 2013;). Massive residences, factories and other industrial or strategic constructions, as well as commercial and touristic activities are among the most inopportune situated places within these zones of high vulnerability in Ecuador and elsewhere (Papathoma et al., 2003; Calgaro & Lloyd, 2008; Calgaro et al., 2014; Barros et al., 2015; Matheus-Medina et al., 2018;).

Therefore, living with the risk has been the common policy of Ecuador, when applying risk assessment measures towards natural hazards of hydro-meteorological or geologic origin, such as floods, droughts, hydric deficit, climate change, mass movements and landslides, volcanic activities, earthquakes and especially tsunamis (Toulkeridis et al. 2007,

Padrón et al., 2008; Ridolfi et al., 2008; Padrón et al., 2012; Toulkeridis et al., 2015a; b; Toulkeridis et al. 2016; Vaca et al., 2016; Rodriguez et al., 2017; Toulkeridis and Zach, 2017; Mato and Toulkeridis, 2017; Jaramillo Castelo et al., 2018; Zafrir Vallejo et al., 2018; Aguilera et al., 2018; Palacios Orejuela, and Toulkeridis, 2020; Toulkeridis et al., 2020a; b; Poma et al., 2020). Nonetheless, due to the last catastrophic events, such as the earthquake of 2016 and the volcanic crisis of 2015, Ecuador´s policy started to change from a passive way of reacting to disasters after their occurrence towards a more proactive risk assessment, improved and more controlled land use management, signage of evacuation routes, drilling of the population and preventive education as well as even mitigation structures where affordable prior potential impacts (Toulkeridis, 2016; Toulkeridis et al., 2020c; Yépez et al., 2020; Herrera-Enríquez et al., 2020). In case of the coastal part of Ecuador, a high amount of tsunami evacuation signs have been installed, although many more are needed, while several are inadequately placed, indicating a longer than needed path towards safety among other issues (Celorio-Saltos et al., 2018; Matheus-Medina et al., 2018).

Furthermore, evacuation routes may be often too long in order to arrive safe in case of a short-time warning of a tsunami (Matheus Medina et al., 2016; Rodriguez et al., 2016; Toulkeridis et al., 2017a). For this specific situation, buildings with a sufficient amount of floors may be used for a vertical evacuation as a temporary shelter (Yeh et al., 2005; Park et al., 2012; Matheus Medina et al., 2016; Mostafizi et al., 2019). Such buildings however, need to be resistant themselves towards telluric movements of high intensity or magnitude as well as for the impact of the incoming waves of tsunamis (Lukkunaprasit & Ruangrassamee, 2008; Meyyappan et al., 2013; Navas et al., 2018; Belash & Yakovlev, 2018; Aviles-Campoverde et al., 2021).

Based on the aforementioned aspects, the current study has been applied within a high frequented touristic village in Ecuador, where an evaluation of the resistance of seismic movements and tsunami impacts of temporal shelters shall indicate, which of these buildings are conformably assigned to stand as a safe area for the evacuating public. Such evacuation has been based on a formal analysis of escape times and routes as well as potential tsunami impact scenarios and modeled wave heights. This pioneering investigation based on international criteria may serve as an example of contemporary risk assessment and management which allows a better relationship and compatibility between existing hazard zones and a corresponding land use policy in the coastal area of Ecuador.

2. GEODYNAMIC SETTING AND STUDY AREA

Tsunamis with some devastating results, originated from the local, regional and far geodynamic environments prone to hit the Ecuadorian coastal areas and its relatively unprepared population as well as their settlements, which are situated within an active continental margin (Pararas-Carayannis, 1980; Herd et al., 1981; Kanamori & McNally,

1982; Mendoza & Dewey, 1984; Pararas-Carayannis, 2012; Ioualalen et al., 2011; 2014; Chunga & Toulkeridis, 2014; Heidarzadeh et al., 2017). The coastal continental platform of Ecuador is situated along the Pacific Rim and therefore within an area which is impacted regularly by tsunamis due to a severe earthquake activity (Gusiakov, 2005; Pararas-Carayannis, 2012; Rodriguez et al., 2016). The geodynamic constellation results from the subduction of the oceanic Nazca Plate (together with its above situated Carnegie Ridge) below the continental South American and Caribbean Plates, which are both separated by the Guayaquil-Caracas Mega Shear (Fig. 1; Kellogg et al., 1995; Gutscher et al., 1999; Egbue and Kellog, 2010). This active continental margin give rise to a variety of tsunamis of tectonic as well submarine landslide origin (Moberly et al., 1982; Pontoise and Monfret, 2004; Ratzov et al, 2007; 2010; Ioualalen et al., 2011; Pararas-Carayannis, 2012). Furthermore, tsunamis or even iminamis may be generated by massive sector collapses of volcanoes in the Galapagos archipelago (Kates, 1976; Cannon, 1994; Keating & McGuire, 2000; Pararas-Carayannis, 2002; Whelan & Kelletat, 2003; McGuire, 2006; Glass et al., 2007; Pinter & Ishman, 2008; Toulkeridis, 2011).

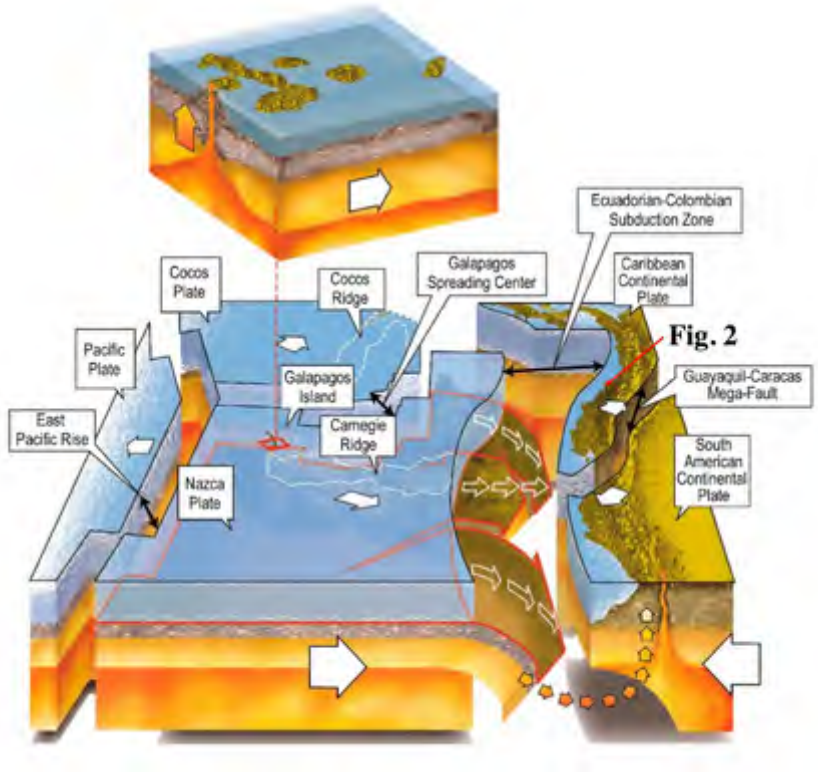

Fig. 1. Geodynamic setting of Ecuador with associated oceanic and continental plates and a variety of plate boundaries, such as the divergent plate boundaries named East Pacific Rise and Galapagos Spreading Center, the convergent plate boundary represented by the Ecuadorian-Colombian Subduction zone, as well as the transcurrent plate boundary represented by the Guayaquil-Caracas Mega-Fault. Also shown the Galapagos Islands and the Carnegie Ridge. Adapted from Toulkeridis, 2013, modified of Toulkeridis et al., 2017a.

Due to the aforementioned geodynamic setting, Ecuador has been impacted by several seismic and tsunami hazards, based on the occurrence of local earthquakes, such as on January 31, 1906 (8.8 Mw), October 2, 1933 (6.9 Mw), May 14, 1942 (7.8 Mw), December 12, 1953 (7.3 Mw) , January 16, 1956 (7.0), January 19, 1958 (7.6 Mw), December 12, 1979 (8.2 Mw), August 4, 1998 (7.2 Mw) and April 16, 2016 (7.8 Mw), besides other less intense occurrences (Berninghausen, 1962; Kanamori and McNally, 1982; Pararas-Carayannis, 2012; Chunga and Toulkeridis, 2014; Toulkeridis et al., 2017a; 2017b; 2018). Besides the short time impacts of local tsunamis, Ecuador has been also the target of distant origin tsunamis, like the one generated in Japan on March 11, 2011 (8.9 Mw), which resulted to a considerable run-up in the Galápagos islands and the Ecuadorian mainland (Simons et al., 2011; Norio et al., 2011; Rentería et al., 2012; Lynett et al., 2013).

The study area comprises the city of Bahía de Caráquez, which is situated on the northern coastal area of the Province of Manabí, and is considered one of the most beautiful and picturesque sites of the entire country due to its interesting landscape and its contact with the ocean. The characteristic of this city is that of having a sinuous morphology, with hills of medium to high heights and also flat areas, being almost at sea level, which correspond to terraces of the Chone River and to deposits of sand accumulation of fluvio-marine origin (Fig. 2).

Fig. 2. Geographic setting of the study area with the city of Bahía de Caráquez, next to the village of San Vicente, separated by the Chone River. Width of image is about 17 km.

Low, practically flat areas could be severely damaged with the occurrence of a tsunami, as the waves would practically pass from one side to the other on the shoreline. Such flat area is currently occupied by a modern and important physical infrastructure, since this sector is the one with the highest added value, where also the tourist potential of the city is

Fig. 3. The city of Bahía de Caráquez with some important elements such as road network, hotels, educational institutions and other strategic buildings

concentrated. The hilly sector has been occupied by poor settlements, therefore the infrastructure is of low quality (mixed constructions), with almost no basic services, with the exception of electricity. In addition, the flanks of the hills are very unstable, especially in the rainy season and within seismic stresses. The accesses to the hilly sector lack to be easy due to the strong inclination of the land, its unstable slopes, its occupation and the vegetation cover. There are few roads to enter the sector, which are built for community purposes (access to drinking water storage tanks, radio and telephone transmission antennas, etc.), and extensive and intricate bleachers for the use of the inhabitants of this elevated sector area (Fig. 3; Barrio La Cruz, next to Mirador La Cruz).

The flat part of the city of Bahía de Caráquez is built on clastic sediments (clay and sandstone) of Miocene to the Pliocene ages, which belong to the Onzole and Borbón Formations (Stainforth, 1948). However, a large part of the extreme seaward side is built on top of fillings which stretched the city to the Lighthouse (El Faro) of the past (Fig. 3, 4). The city recently suffered great damage with the earthquake of August 4, 1998 (7.2 Mw), which epicenter was barely 3 km from the center of the city, with the far-distant tsunami of March 11, 2011 of Japan with slight damages, and lately with the earthquake of April 16, 2016 (Mw 7.8) with the epicenter about 105 km to the north (Pararas-Carayannis, 2011; Toulkeridis et al., 2017b; Morales et al., 2018; Chunga et al., 2019a; b). The city counts with some 57,159 permanent citizens, with a population density of 143.55 persons per km^2. An important strategic element of the city is represented by the largest bridge of the country, called “Los Caras” (Fig. 3, 5). This bridge which connects Bahía de Caráquez with San Vicente was constructed in 2010 and counts with seismic isolators (Aroca et al., 2018).

Fig. 4. Note in the image of 1960 the distance of the old Lighthouse and the main city of Bahía de Caráquez, which was later filled and the city extended.

In the peninsula of Bahía de Caráquez the tropical Savanna climate predominates, to the north the climate changes to tropical monsoon. The Savanna-type climate presents a marked dry trend between June and November, as well as a trend of rain or winters between January and April. In winter, there is greater wear on the ground cover and a greater flow of debris descending the slope, where some houses may collapse.

Fig. 5. Aerial panoramic view of Bahía de Caráquez, from north to south. Left side is the estuary of the Chone River, as well as part of the San Vicente – Bahía bridge and towards the right side is the Pacific Ocean.

The collapsed buildings in Bahia are directly related to the types of soils, which are colluvial that covered paleo-fluvial channels, where the amplifications of the seismic waves lasted longer. Other types of mainly sandy soils may also occur in the coastal plain zone. Geological field reconnaissance (Fig. 6) has allowed to corroborate the geomechanical behavior and instability of the slope, in fact, rotational and translational landslide escarpments have movement trends along the axis of the river tributaries. The easy disintegration of the rocky substrate by the runoff waters increases the openings of the traction cracks and forms subsequent collapses of silt strata. It should be noted that these strata have joints or cracks, which are filled and placed by plaster or gypsum. In several homes in the upper part of the La Cruz de Mirador site, multiple traction cracks are able to be seen with openings that reach between 15 and 30 cm, while their opening dimensions decrease when approaching the street, where there are cracks between the 10 to 15 cms. The distances between cracks are in the order of 0.8m, 1m, 1.4m and 1.6 meters apart.

Evidence of potentially active quiescent landslide escarpments are located in the frontal part near the Cruz del Mirador. From a structural geological analysis point of view, they tend structurally in the same direction N100° to N110°, being the same tendency to the inclination of the slope, which makes it a site with a high level of instability. The soil layer and colluvial slope material are vertically displaced by a recent rotational-type sliding escarpment in a quiescent manner, where the vertical displacement is 40 cm high, with a trend of N100° running parallel to the direction of the inclination of the slope. This structural guideline has a bearing trend of N12°.

Unstable geological features of cracks and landslide escarpments were already evident at the Cruz del Mirador site, when in 1999 the first houses began to be built in this upper part of the city of Bahía de Caráquez. In 2013, the houses already reported damage to their walls and floors, and the back part already showed signs of detachment due to being in an area of unstable natural slope. During the earthquake of 1998, in the La Cruz del Mirador sector, 56 homes that already had a record of minor damage that were left uninhabitable, collapsed during the strong earthquake of April 16, 2016 (Mw 7.8).

Fig. 6. Delineation of river sub-basins (yellow lines) characterized by intermittent streams, active only in winter seasons and "El Niño" phenomenon, and formation of deep furrows by incision of runoff waters on the slope, around the lower part of the "Mirador" de la Cruz site.

3. METHODOLOGY

a) Evaluation of wave heights and potential impact scenario

In this research, we use the extensively validated tsunami modelling tool, the ComMIT/MOST model (Community Model Interface for Tsunami), which is an internet-enabled interface to the community tsunami model developed by the NOAA Center for Tsunami Research (NCTR). This interface let one run the MOST model (Method of splitting tsunami), a non-linear shallow water model, which has been extensively validated from field observations and laboratory experiments (Fig. 7; Titov et al., 2011; Titov et al., 2016).

We have created a numerical domain for the coordinates [-0.7510 , -0.3868] [-80.7862 , -80.2887], a grid size of [598 x 438], with a raw resolution of 3 arcsec (~92.8 meters). This

is a very constraint resolution, since it limits one to differentiate the change between sea and land, and also affects the performance of the flooding algorithm of the model. The lack of high-resolution information of this area, should be considered as a constraint. This particular behavior in global bathymetry datasets, has been extensively discussed in Griffin et al., 2015.

Considering the geodynamic settings and the hazard evaluation regards to potential earthquakes in this area, we simulated a 8 Mw earthquake , which is greater than the

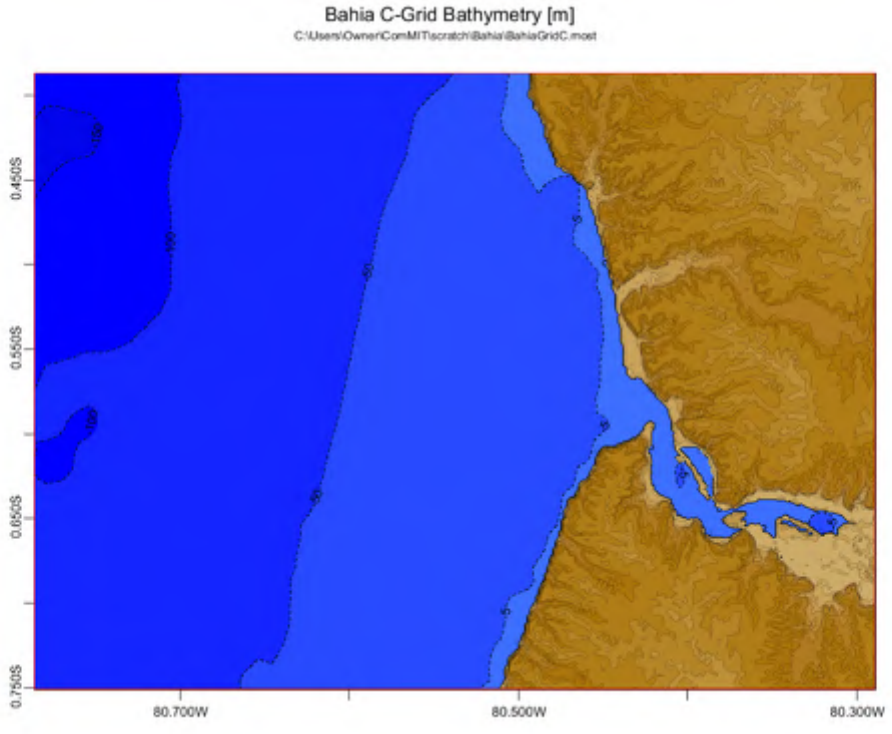

Fig. 7. Grid bathymetry for the area of interest, taken from global dataset, based on Commit/Most app.

historic events, but let us cover the lack of reliable information in the for the national catalogue about earthquakes. Based on this model, we are able to evaluate the potential model with the corresponding wave amplitude, and not the run up (Intergovernmental Oceanographic Commission, 2019). It is important do not confuse the wave amplitude with the run up, the latter is the maximum height of the water running into the land, but as we mentioned before, the data resolution constraint of ours results, in this case limiting to have a good information in horizontal flooding (Fig. 8).

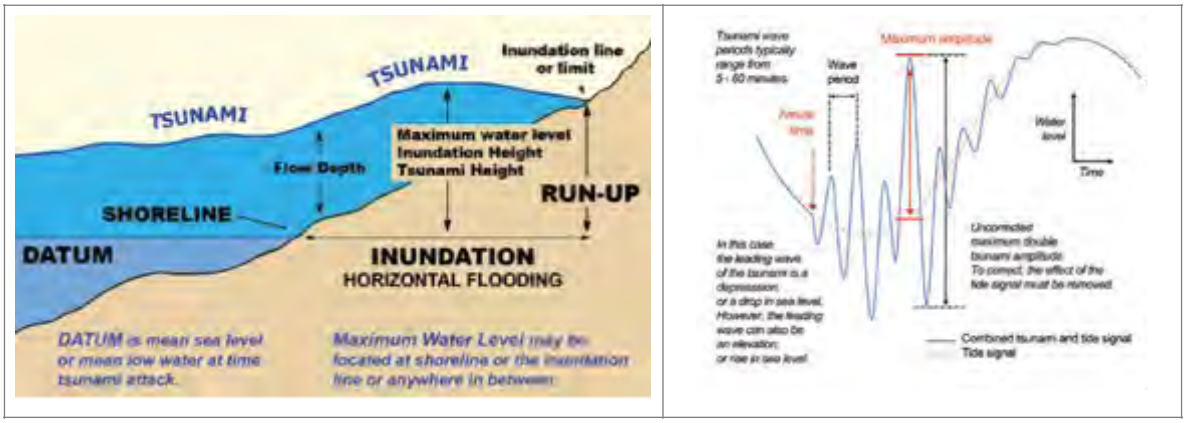

Fig. 8. Definition of Tsunami Run up and Tsunamis amplitude (Intergovernmental Oceanographic Commission, 2019

b) Analysis of evacuation times and routes

Almost independent of the arrival times of tsunami waves, the population involved in this area needs to be evacuated when the phenomenon occurs. With this criterion, a safety distance was taken for the inhabitants of about 50m in the periphery of the potential tsunami waves, which means in a necessary margin in which the population needs to mobilize outside such sector. In other words, the flood areas were taken unifying them in a single polygon with a buffer of 50m around it, calling it the Safety Zone (SZ). The 50 meters has been decided taking as an element that offers a margin of safety that would allow anyone to escape from this area. This was decided based on safety criteria adopted from previous experiences (Saji, 2014; Wood et al., 2014; Mostafizi et al., 2019).

Hereby, for the analysis it is essential to define three elements for calculating evacuation times: safety points, evacuation points and road axes (Fig. 9). Taking the road network, the road axes were intersected with the SZ. Each of the points that are at the end of the road axes and on the edge of the SZ are the Security Points (SP). To define the Evacuation Points (EP), points were taken along the road axes located every 20 meters, which corresponds to an approximate distance between the portals of each of the houses. Subsequently, the model will be run with more precise data with points located in each portal of the homes in the study area.

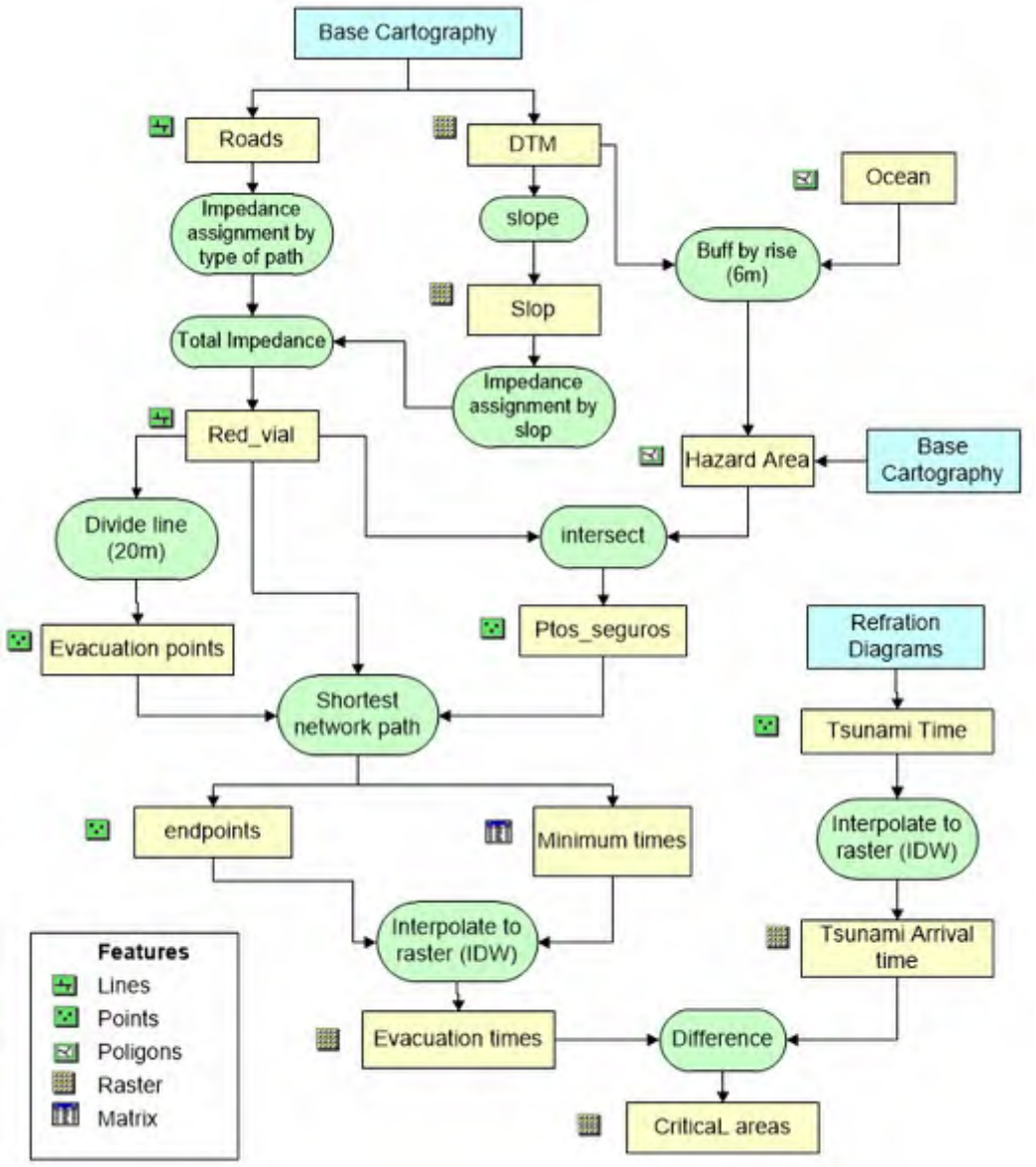

Figure 9. Methodology used in the evaluation and generation of evacuation times and routes

With these three elements SP, EP and Road Axes, the distances between each of the points of origin (EP) to each point of arrival (SP) were calculated (Fig. 10). This problem may have some possible solutions, the simplest taking into account the distances of each of the arcs between the two points. In the current study, the value multiplied by the distance of each of these segments was considered as impedance. The impedance values in each one of the roads were assigned fundamentally with the times of vehicular circulation in peak hours. The possibilities may vary only depending on the type of problem you are planning to solve. The solution could be expressed in the following equation:

$$\mathbf{Dc = DistMin\ ij\ (\Sigma dijk * Iijk)}$$

Where:

Dc	Solution or shortest path
DistMin ij	Selection function of the minimum value between points i and j
dijk	distance of each of the arcs of the network k
Iijk	impedance value of each arc in the network

The solution possibilities of this expression, depends on the initial conditions of the network and the specific problem to be solved. The total number of data can be very large, so the Shortest Network Path subroutine was used as a calculation aid, which was loaded in the ArcView 3.2 platform™, taking the total databases and selecting the lowest times in each of the routes. This database was linked to the EP elements, obtaining a map of points with the smallest values of evacuation time and the point towards which they should escape to (SP).

As mentioned, the ideal is that each portal becomes an evacuation point with information on use and number of people who live, for this it is necessary to perform the calculations with bases of the most current data and with a Workstation with good processing characteristics (Fig. 11). This point database was used to generate the Evacuation Time Map, which was calculated using the inverse distance interpolation model (IDW), which in this case gives better results because the variable that needs to be calculated must have a spatial continuity or in this case temporal, obtaining the Map of evacuation times.

The map of first wave times (Fig. 14), corresponds to the tsunami arrival times obtained in minutes, over the different zones of the work area. It contains information of a polygonal type with times in integer values, corresponding to a variable of a discrete type. For the subsequent comparison between evacuation times and times of the first wave, it is necessary that these variables be continuous, in addition, this will allow a better

cartographic representation. The previously digitized time map was taken, transforming the polygons into lines and selecting the cut segments between each unit time range, assigning it the same value in the database, for later by interpolation (ArcGis™ IDW) in order to obtain the map of arrival times of the first wave of the potential tsunami.

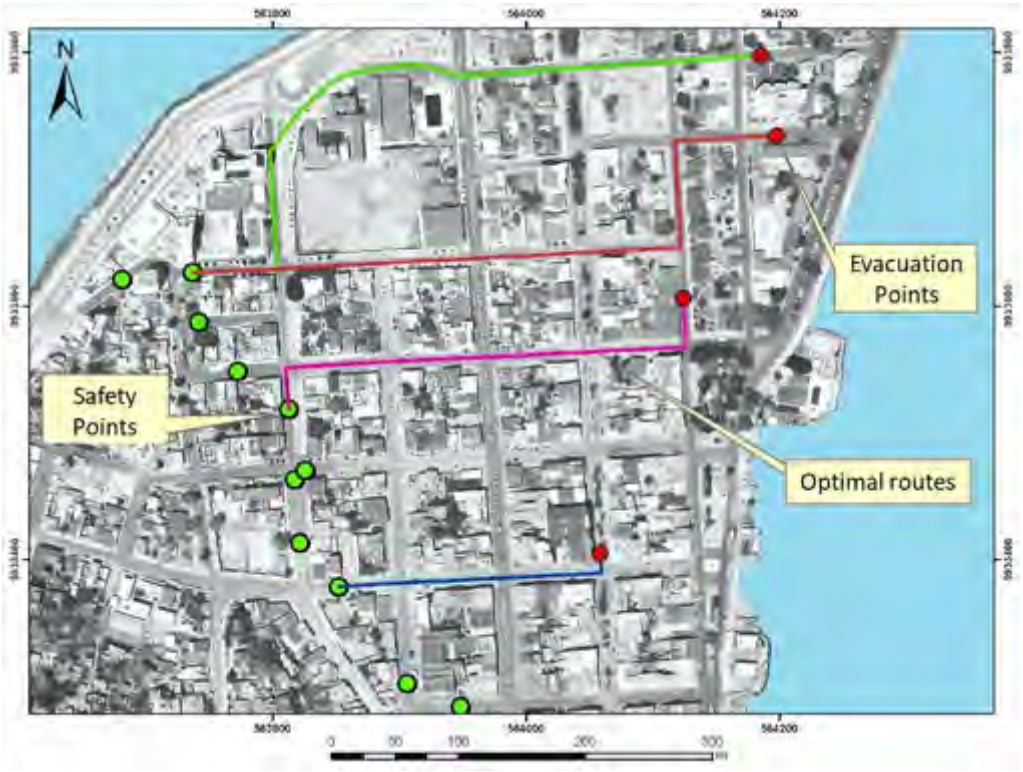

Figure 10. Evacuation and safety points along the potential most optimal routes

Figure 11. Main part of the flooded area and the analysis of given evacuation points.

With the evacuation times and first wave arrival times maps (Fig. 14), a map of time differences between the two was obtained. All positive values indicate areas in which evacuation times are greater than the arrival times of the first wave (the warning time of the first wave is not yet taken into account, based on a still uninstalled early warning system). In the map of Fig. 15 the time differences are illustrated, in which only the areas in which the values are positive (areas in conflict) are indicated, although a greater margin should be taken considering the areas where the values are close to 0 (zero).

$Te - Tpo \geq 0$ Conflict area
$Te - Tpo \approx 0$ Areas with approximately equal times
$Te - Tpo \leq 0$ Areas with shorter evacuation times

Where:
Te corresponds to evacuation time
Tpo corresponds to arrival time of the first wave

However, an additional objective has been to encounter some ways to represent these variables with a simple and intuitive cartographic language that can be understood by all those involved in the phenomenon, that is, from a technical specialist to any member of the affected population in the area, therefore the representation was chosen to be by three-dimensional variables. In order to represent different variables in the same vector space, it is necessary that they lie on the same plane (thematic variables) or the same units (heights). In this case, the aim was to represent basically two different types of variables in a three-dimensional space: time and heights. It is clear that both are on different scales and units. A simple representation solution resulted in normalizing the variables (Carver, 1991). This allowed the variables of time (minutes) and elevation (masl) to be represented in the same view.

In evacuations realized in buildings, it is estimated that an adult without physical impediments has a horizontal displacement speed of one meter per second, which would be equal to 60 meters in 1 minute (Thompson & Marchant, 1995; Zhong et al., 2008; Tsai et al., 2011). However, to calculate the evacuation times in the present work, a displacement speed of 50 meters per minute was assigned, considering that the population to evacuate includes children and the elderly. In order to calculate the evacuation times, the minimum roads calculation routine was used, using as initial data the population displacement speed of 50 meters per minute, using the following equation, for each segment of the road network (Cheng et al., 2011; Zhang et al., 2016; Sun et al., 2017).

$$Time = \frac{Impedance * Length}{Velocity}$$

In turn, with the evacuation times obtained, the critical area was calculated, that is an area in which people will not have enough time to evacuate. In such area the evacuation times are greater than the arrival times of the incoming tsunami (Fig. 15).

c) Criteria used for seismic and tsunami resistance evaluation of potential provisional shelters

A total of 26 buildings along the coastline of Bahía de Caráquez were evaluated for their seismic as well as tsunami resistance (Fig. 12) in order to assess their feasibility as provisional shelters for vertical evacuation in case of an impact by a tsunami (Fig. 9). The pre-selection of buildings was performed according to their height, considering those with more than four floors, based on the own calculation and modeling of an incoming tsunami to have a height of at least six meters. The evaluation of each building was performed by couples with civil engineering expertise in order to minimize the subjectivity.

Fig 12. Map with the location of the 26 evaluated buildings

First, general data were collected such as name of the building, geographical location, address, total number of floors, number of floors below and above surface, average altitude of each floor, area and year of construction, current use as well as capacity. After this initial part, an evaluation was performed in order to reveal the seismic resistance of each building, by using twelve criteria based on the Modified Italian Methodology in order to calculate the seismic vulnerability index (SVI) (Table 1; Calvi et al., 2006; Amellal et al., 2012; Kassem et al., 2019).

Table 1: Modified Italian Methodology to calculate the SVI (Aguiar&Rivas, 2018)

Criteria	**Classes / Ki**			Weighting **Wi**
	A	**B**	**C**	
1. Organization of the resistant system	0	6	12	1,00
2. Quality of the resistant system	0	6	12	0,50
3. Conventional Resistance	0	11	22	1,00
4. Position of the building and foundations	0	2	4	0,50
5. (Floor)Slab	0	3	6	1,00
6. Floor configuration	0	6	12	1,00
7. Configuration in Elevation	0	11	22	1,00
8. Connection in critical elements	0	3	6	0,75
9. Low ductility elements	0	6	12	1,00
10. Non-structural elements	0	4	10	0,25
11. State of Conservation	0	10	20	1,00
12. Structure reinforced after earthquake	0	11	22	1,00

Furthermore, we added an additional evaluation, for the corresponding tsunami resistance of each building (Table 2). Hereby, the tsunami evaluation contained ten criteria which were defined by following the Guidelines for Design of Structures for Vertical Evacuation from Tsunamis of the Federal Emergency Management Agency of the United States of America (FEMA, 2019).

Table 2. Methodology to calculate the tsunami vulnerability index

Criteria	Classes / Ki			Weighting **Wi**
	A	**B**	**C**	
1. Building orientation	0	6	12	1,2
2. Access. Entrance	0	6	12	1,2
3. Access. Stairs	0	6	12	1,2
4. Building location. Potential hazards	0	6	12	0,5
5. Building location. Parking, traffic, streets	0	6	12	0,5
6. Structural system	0	6	12	1,00
7. Foundation system	0	6	12	0,5
8. Year of construction	0	6	12	1,00
9. Building Height	0	11	22	1,50
10. Floor system	0	6	12	1,00

In both the seismic and the tsunami evaluation of vulnerability, each criteria was classified in three vulnerability classes, being “A”, “B” and “C”. In this case “A” shall represent the most resistant building, while “C” shall reflect the most vulnerable structure, where each class corresponds to a value (Ki). Furthermore, each criteria was assigned to a fixed weighting coefficient (Wi) according to the importance of the criteria. The total seismic and tsunami vulnerability index for each building was calculated according to the equation:

$$I_V = \sum_{i=1}^{12\,(S)or\,10(T)} K_i\, W_i$$

According to table 1, the maximum value for the seismic vulnerability index is 143 while the maximum value for the tsunami vulnerability index is 130.2 (Table 2). Considering the aforementioned, the following general categorization for vulnerability is proposed:

Resistant structure

if $I_v \leq 30$

Highly vulnerable structure

If $I_v \geq 80$

Further evaluation is needed:

If $30 < I_v < 80$

This occurs especially with the calculation of the ratio between the building height and the vibration period of the structure (Duque Eslava et al., 2017; Aguiar and Zambrano 2018; Rodriguez, 2019).

4. RESULTS AND DISCUSSION

a) Wave height of tsunami

Based on the used Community Model Interface for Tsunami, our results suggest a tsunami weight height from 2 to 3 meters along the coast, which has been computed without the influence of the tide, taking the reference level to the mean sea level. According to the Tide table of INOCAR, we have a tide range of 3 meters, which means that we need plus 1.5 meters due the high tide, then easily the wave amplitude at the coastline should reach the 4.5 meters (Fig. 12). Considering the bathymetry constraint as it has been showed by Griffin et al., 2015, the models results along the coastline, showing the maximum wave amplitude.

b) Evacuation times and routes

Unfortunately, in the entire country of Ecuador and similar to equivalent developing countries, land use with respect to hazards zoning has not been a priority in the state´s policy as eveidenced in several cases (Suango Sánchez et al., 2019; Echegaray-Aveiga et al., 2019; Herrera-Enríquez et al., 2020; Robayo et al., 2020; Zapata et al., 2020; Barreto-Álvarez et al., 2020). Bahía de Caráquez is not an exception, where, in order to extend the city´s land, landfilling has been applied in order to expand the area of construction towards the previously islet of the Lighthouse (El Faro) by incorporating it. This extension, is nowadays an enlargement of the city´s vulnerability towards potential tsunamis and represents additionally an instability in respect to future earthquake shacking. Therefore, logically, in the city of Bahía de Caráquez, the areas furthest from the beaches of Pacific Ocean and the estuary of the Chone River, which correspond to the foothills and the hills themselves, are considered to be relatively safe. Therefore, the inhabitants of the central neighborhoods, located at the foot of the hills, need shorter evacuation times (between 0 to 8 minutes) to reach these sectors (Fig. 12).

The population located in the vicinity of the boardwalk, both in the beach sector and along the river bank, is far from the indicated safety zone, which is approximately 1 kilometer away, so it needs longer evacuation times. This evacuation time is between 16 to 24 minutes, as can be seen in figure 11.

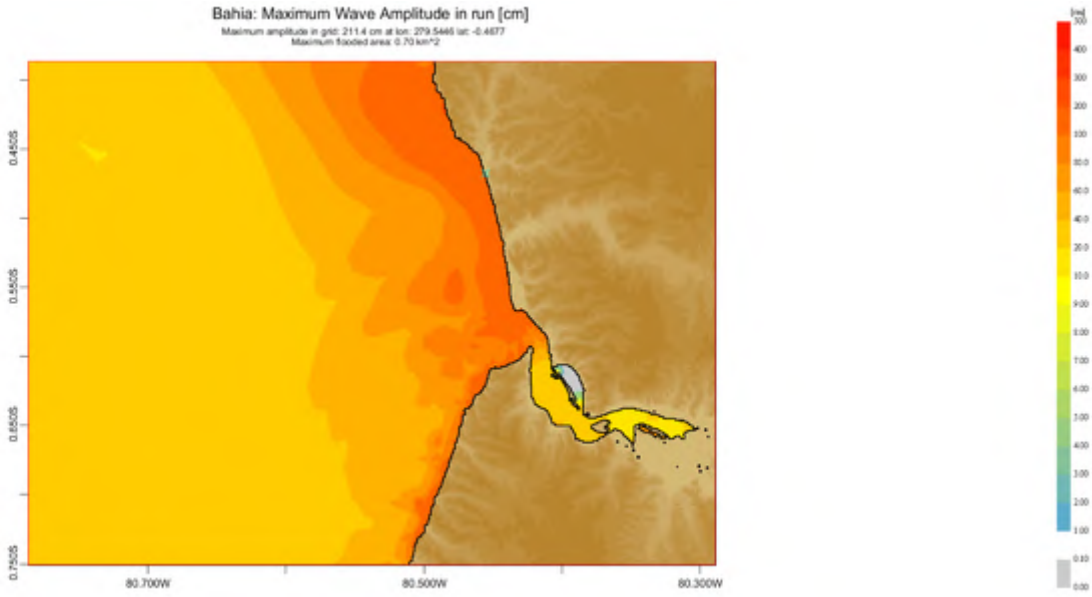

Fig. 12: Maximum Wave Amplitude, MWA, along the coastline cover the Bahia de Caráquez area. Note the MWA is in the range 2-3 meters.

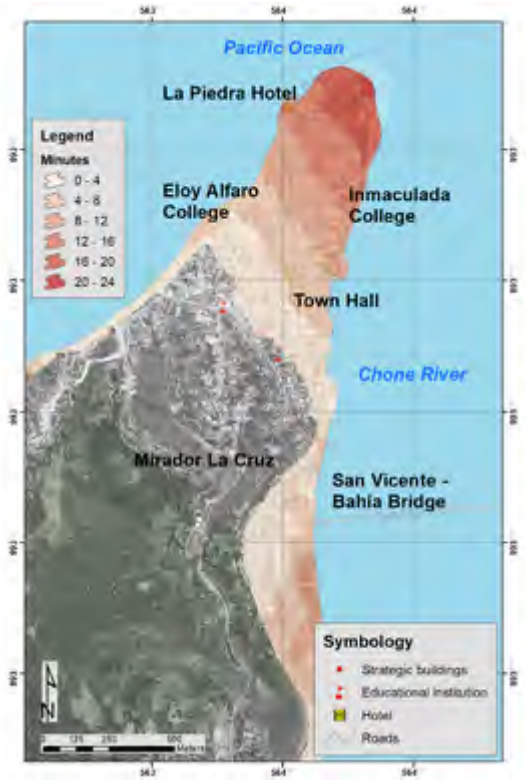

Figure 13. Map with the evacuation times

Figure 14. Map with tsunami arrival times

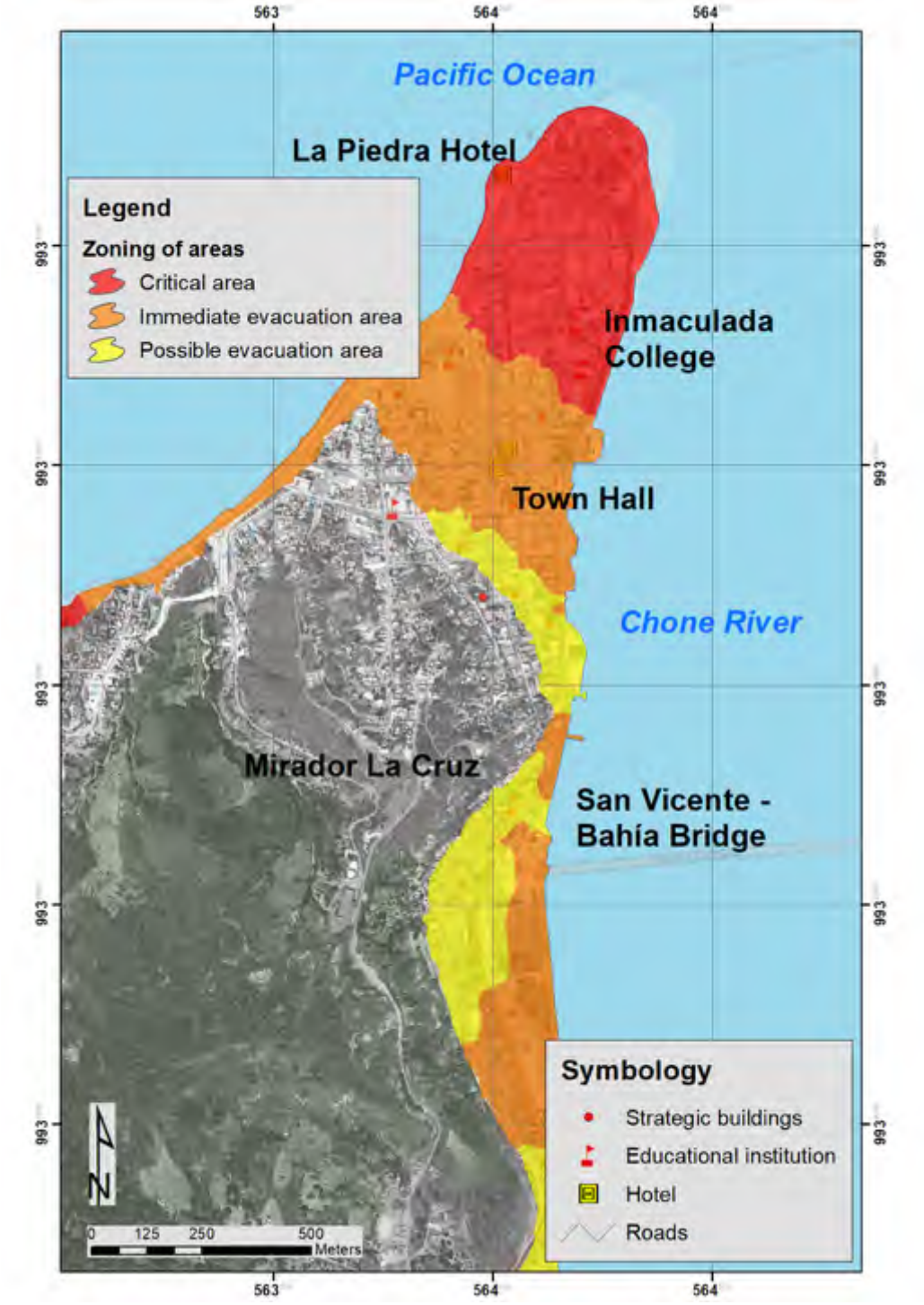

Figure 15. Zoning of areas in respect of the calculated evacuation times of the public and the modeled and calculated arrival times of the potential tsunami.

The times calculated for the arrival of the first wave are in the order of 4 to 12 minutes (Fig. 13). For this reason, the sector next to the Pacific Ocean constitutes a critical area, highly vulnerable, as shown in figure 12. The side of the city that faces the Chone River will also be impacted by the tsunami wave. but a little later than the seaside. The southern part of the city towards the San Vicente - Bahía Bridge will be impacted as the latest part of the incoming tsunami.

Taking into consideration the results of Fig. 13 of the time of the horizontal evacuation together with the results of Fig. 14 of the tsunami arrival times, we elaborated a zoning of the different degrees of vulnerability in form of distinctive areas, being critical areas, areas of immediate evacuation and areas possible evacuation (Fig. 15). Therefore, the only alternative for survival for the population located in critical areas is vertical evacuation in buildings considered earthquake-resistant and also tsunami-resistant, that is, in those in which it is certain that they will not suffer structural damage from effect of the generating earthquake or by the hydraulic effect of the waves, or having vehicles for mass transport of people, which can evacuate towards the upper parts or towards the interior, that is, south of the city, and away from the Chone River, as appropriate.

Furthermore, due to its characteristics, also the "Dos Caras" bridge, which connects San Vicente with the city of Bahía de Caráquez may considered a safe area or site for the incoming tsunami. This bridge, as aforementioned, counts with seismic isolators and has withstand without any damage the most recent 7.8Mw earthquake of 2016, while a variety of buildings collapsed on both ends of the bridge (Toulkeridis et al., 2017b; Aroca et al., 2018).

c) Seismic and tsunami vulnerability assessment of existing buildings

The property status, as well the use, of all the buildings evaluated is private. A high percentage (96.15%) of the 26 buildings are of residential use, and only one of the damaged buildings (# 25) was previously used as a hotel (Fig. 16, 17). As for the year of construction, seventeen (65.38%) of the buildings were constructed prior to the earthquake of 1998 with 1990, 1993 and 1994 as the most frequent years of construction. Another seven were built after the earthquake of 1998, and two more buildings are less than five years old, therefore, those two were built after the Ecuador earthquake (Mw 7.8) of the 16 April 2016. The total area of construction of the 26 buildings sum up to more than 9000 m^2, while the average area of construction is 367,4 m^2. The largest area of construction corresponds to the building Dos Hemisferios (#20) with 1720 m^2 followed by the Centinela (#24) with 1200 m^2 and Ocean Bay Tower (#15) with 710 m^2, a higher area of construction would be related to a higher capacity in case of evacuation. Regarding the total number of floors, most of the buildings, a total of twenty, present eight, nine or ten floors whereas four buildings have less than seven floors. Two buildings reach eleven floors. Only two out of the 26 buildings have one and two floors respectively below the surface.

Concerning the average altitude of each floor, the minimum is 2.4 meters while the maximum is 3.5 meters. Seven buildings show an average altitude of $\leq$ 2.6 meters per floor

whereas four buildings reach more than 3 meters per floor. The most frequent average altitude per floor are 3 and 2.8 meters with nine and five buildings respectively. 22 out of the 26 buildings are located right in the beachfront (Fig.12) and within the critical and immediate evacuation area (Fig.15) Among the 26 buildings evaluated, 4 of them exhibit clear damage and were uninhabited and abandoned, while 3 of them are in their last stage of construction as January 2021.

Figure 16. A: Akuaba (#1); B: Nautilus (#2); C: Albatros (#4); D: Spondylus (#5); E: Capitán (#8); F: Ocean Bay Tower (#15); G: Torre Mariana (#26); H: Dos hemisferios(#20).

Figure 17. A: Agua Marina (#16); B: No name, damaged (#19); C: Sucre (#21); D: Horizonte (#22); E: Las Brisas (#23); F: Hotel Patricio´s (#25).

The building stock exhibits an intermediate overall seismic vulnerability, as the nine resistant structures with vulnerability index (I_v) ≤ 30 account for about 34.61 % in terms of number of buildings, while highly vulnerable buildings with $I_v \geq 80$ sum up five of them. Almost half of the evaluated structures (12, 46.15%) exhibit a seismic vulnerability index between 30 and 80, therefore, further evaluation is needed. The minimum seismic *Iv* is 9 and is achieved by two buildings, being Akuaba (#1) and by the building El Faro (#12). The highest vulnerability index values are performed, as expected, by the four buildings that are already abandoned due to their damage during previous earthquakes (Table 3). Since they could possibly collapse in future earthquakes posing a threat to adjacent buildings and inhabitants, these four buildings should be subject to a controlled demolition.

The distribution of the nine seismic resistant structures is heterogenous across the evaluated area, although a slight higher concentration of four safe buildings could be encountered towards the northeastern tip of the peninsula of Bahía de Caráquez (Fig. 18). Three of those buildings, being Albatros (#4), Torre Mar (#6) and Cariló (#14) are recent constructions from 2019, 2018 and 2015 respectively, whereas Mykonos is an exception for being an older construction from 1993.

Table 3: Summary of seismic and tsunami vulnerability index (Iv)

Building	Seismic Index	Tsunami Index
1-Akuaba	9.00	43.8
2-Nautilus	42.00	39.6
3-Torre Molinos	38.25	52.2
4-Albatros	28.25	34.2
5-Spondylus	43.50	52.8
6-Torre Mar	14.00	40.8
7-Mykonos	26.00	32.4
8-Capitán	43.25	58.5
9-Vista Mar	48.50	49.8
10-Neptuno	54.75	48.6
11-Punta Norte	105.25	72.0
12-El faro	9.00	37.8
13-Las Gaviotas	56.75	69.8
14-Cariló	18.00	20.4
15-Ocean Bay Tower	34.00	36.6
16-Agua Marina	34.00	36.6
17-El Pirata	12.00	58.2
18-Torre Sol	93.25	64.2
19-No Name, damaged	95.25	68.0
20-Dos Hemisferios	45.50	48.6

21-Sucre	49.00	30.6
22-Horizonte	19.00	46.8
23-Las Brisas	126.50	73.0
24-Centinela	26.00	40.8
25-Hotel Patricio´s	116.50	75.6
26-Torre Mariana	54.00	36.6

All of the buildings evaluated, except one, exhibit a tsunami vulnerability index (I_v) between 30 and 80, hence, require further evaluation for tsunami resistance. None of the structures reach $I_v \geq 80$. Only one out of 26 buildings is categorized as a tsunami resistant structure with $I_v \leq 30$, being the building Cariló (#14) with a TVI of 20.4. However, another seven buildings indicate tsunami vulnerability indexes below 38 being moderately close to the tsunami resistant category (Table 3).

Therefore, when assessing together the seismic and tsunami vulnerability indexes, only one building is categorized as resistant to both hazards and could be considered for vertical evacuation in case of tsunami impact. Building Cariló (#14) is the only structure with Iv lower than 30 for both the seismic and tsunami assessments, which seems to be related to a combination of attributes including that it was built in 2015 following the stricter building standards established in the Ecuadorian Code of Construction (NEC), hence, it did not suffer structural damage at all when it was hit by the earthquake of 2016 (NEC, 2015). The structural attributes that allows to be Cariló a resistant seismic and tsunami building include a strong and well organized system with reserve capacity to resist extreme forces as well as an adequate connection in critical elements.

Furthermore, the long direction of Cariló is oriented parallel to the most potential direction of the incoming tsunami wave from the Pacific coast, hence, it will experience smaller hydrodynamic forces. It is one of the few buildings evaluated which is not in the beachfront but in a second beach line, and features a large entrance from a wider street than the street right by the estuary where buildings #6 to #12 are located. Overall, Cariló is located in the critical tsunami area (Fig. 15 and 18) and could serve to evacuate around 200 people thanks to its ten floors of height, and the amplitude of its construction area (600 m^2).

Moreover, we propose physical adaptations to improve the vertical circulation to the appropriate shelter level of the structure such as installation of supplemental entrances, ramps, and stairs. In order to facilitate the construction, and provide unobstructed access with high visibility, the auxiliary ingress could be placed in the exterior of the structure (FEMA, 2019). As a further option, the city of Bahía de Caráquez should consider the design and construction of a public and accessible multipurpose tsunami resistant building in the central area of the critical zone (Fig. 15) equidistant to the hilly sector and the Cariló

building, which could serve to evacuate the people who could reach neither the hills nor the Cariló. All of the proposed activities in case of a potential disaster by an incoming tsunami are pending of the implementation of an early alert system as previously proposed (Toulkeridis et al., 2018; 2019).

Fig.18. Maps representing the three categories assigned to seismic and tsunami vulnerability of the evaluated buildings. Green: Resistant structure with $I_v \leq 30$; Orange: Further evaluation is needed with $30 < I_v < 80$, and Red: Highly vulnerable structure with $I_v \geq 80$.

5. CONCLUSIONS

The population and the tourists of the city of Bahía de Caráquez have only a limited time to reach an elevated, safe area in case of an incoming tsunami. Such area would be the hilly, southern part of the city.

Based on the vulnerability evaluation of seismic and tsunami resistance of the 26 existing buildings along the Chone river and the beachside towards the Pacific Ocean, we may ascertain that many of the buildings could withstand a seismic event and most potentially an impact by a tsunami.

The 26 evaluated buildings have a limited if any capacity of obtaining the escaping public in case of an incoming tsunami, as being almost all in private property, lack to allow

other than residents to enter the buildings and perform a vertical evacuation. Although currently only one building is considered suitable as potential tsunami shelter, other buildings could improve their tsunami performance if access is improved, ideally through external adaptations.

It is necessary to implement an early alert system for tsunamis and have an agreement between municipality and owners of the buildings which will allow the escaping public and tourists to enter the buildings and stay safe in elevated floors during a tsunami crisis.

6. REFERENCES

Aguiar, R. & Rivas, A. (2018). Microzonificación sísmica de Ambato. Gobierno Autónomo Descentralizado de Ambato, Ambato, Ecuador.

Aguiar, R. & Zambrano, V. (2018). Relation h/t in structures of Bahía de Caraquez and the 2016 Earthquake. Revista Internacional de Ingeniería de Estructuras, 23, 2, 227-241

Aguilera, C., Viteri, M., Seqqat, R., Ayala, L., Toulkeridis, T., Ruano, A., & Torres, M. (2018). Biological impact of exposure to extremely fine-grained volcanic ash. Journal of Nanotechnology, Article number 7543859

Alcántara-Ayala, I. (2002). Geomorphology, natural hazards, vulnerability and prevention of natural disasters in developing countries. Geomorphology, 47(2-4), 107-124.

Amellal, O., Bensaibi, M., & Grine, K. (2012). Seismic vulnerability index method for steel structures. In Proceedings of the 15th World Conference on Earthquake Engineering (WCEE).

Aroca, J., Gómez, M., Morales, E., & Romo, M. (2018). Study of the performance of seismic isolators of Pier no. 12 of the Bridge "Los Caras", during the earthquake of April 16. Revista Internacional de Vol, 23(3), 305-339.

Aviles-Campoverde, D., Chunga, K., Ortiz-Hernández, E., Vivas-Espinoza, E., Toulkeridis, T., Morales-Delgado, A., & Delgado-Toala, D. (2021). Seismically induced soil liquefaction and geological conditions in the city of Jama due to the Mw7.8 Pedernales earthquake in 2016, NW Ecuador. Geosciences, 11, 20

Barreto-Álvarez, D.E., Heredia-Rengifo, M.G., Padilla-Almeida, O. & Toulkeridis, T. (2020). Multitemporal evaluation of the recent land use change in Santa Cruz Island, Galapagos, Ecuador. In Conference on Information and Communication Technologies of Ecuador (pp. 519-534). Springer, Cham.

Barros, J. L., Tavares, A. O., Santos, A., & Fonte, A. (2015). Territorial vulnerability assessment supporting risk managing coastal areas due to tsunami impact. Water, 7(9), 4971-4998.

Belash, T. A. & Yakovlev, A. D. (2018). Seismic stability of a tsunami-resistant residential buildings. Magazine of Civil Engineering, 80(4).

Berninghausen, W.H. (1962). Tsunamis reported from the west coast of South America 1562-1960. Bull. of the Seismological Soc. of America, 52 (4): 915-921.

Calgaro, E. and Lloyd, K. (2008). Sun, sea, sand and tsunami: examining disaster vulnerability in the tourism community of Khao Lak, Thailand. Singapore Journal of Tropical Geography, 29(3), 288-306.

Calgaro, E., Dominey-Howes, D., & Lloyd, K. (2014). Application of the Destination Sustainability Framework to explore the drivers of vulnerability and resilience in Thailand following the 2004 Indian Ocean Tsunami. Journal of Sustainable Tourism, 22(3), 361-383.

Calvi, G. M., Pinho, R., Magenes, G., Bommer, J. J., Restrepo-Vélez, L. F., & Crowley, H. (2006). Development of seismic vulnerability assessment methodologies over the past 30 years. ISET journal of Earthquake Technology, 43(3), 75-104.

Cannon, T. (1994). Vulnerability analysis and the explanation of 'natural' disasters. Disasters, development and environment, 1, 13-30.

Carver, S. J. (1991). Integrating multi-criteria evaluation with geographical information systems. International Journal of Geographical Information System, 5(3), 321-339.

Celorio-Saltos, J.C., García-Arias, J.M., Guerra-Luque, A.B., Barragan-Aroca, G., & Toulkeridis, T. (2018). Vulnerability analysis based on tsunami hazards in Crucita, central coastal of Ecuador. Science of Tsunami Hazards, 38(3): 225-263.

Cheng, C., Qian, X., Zhang, Y., Wang, Q., & Sheng, J. (2011). Estimation of the evacuation clearance time based on dam-break simulation of the Huaxi dam in Southwestern China. Natural Hazards, 57(2), 227-243.

Chunga, K. & Toulkeridis, T. (2014). First evidence of paleo-tsunami deposits of a major historic event in Ecuador. Science of tsunami hazards, 33: 55-69.

Chunga, K., Mulas, M., Alvarez, A., Galarza, J., & Toulkeridis, T. (2019a): Characterization of seismogenetic crustal faults in the Gulf of Guayaquil, Ecuador. Andean Geology, 46(1): 66-81.

Chunga, K., Livio, F.A., Martillo, C., Lara-Saavedra, H., Ferrario, M.F., Zevallos, I., & Michetti, A.M. (2019b). Landslides Triggered by the 2016 Mw 7.8 Pedernales, Ecuador Earthquake: Correlations with ESI-07 Intensity, Lithology, Slope and PGA-h. Geosciences, 9, 371.

Chunga K., Livio F., Mulas M., Ochoa-Cornejo, Besenzon D., Ferrario M., & Michetti AM. (2018). Earthquake ground effects and intensity of the 16 April 2016, Mw 7.8 Pedernales Earthquake (Ecuador): implications for the source characterization of large subduction earthquakes. Bulletin of the Seismological Society of America 108 (6): 3384-3397.

Chunga, K., Toulkeridis, T., Vera-Grunauer, X., Gutierrez, M., Cahuana, N., & Alvarez, A. (2017). A review of earthquakes and tsunami records and characterization of capable faults on the northwestern coast of Ecuador. Science of tsunami hazards, 36: 100-127.

Duque Eslava, A.C.,Rojas Mendoza, F. A., Rodríguez Gómez, H., & Vielma Pérez, J.C. (2017). Analysis of outer RC beam-column joint strengthened with CFRP. Revista Internacional de Ingeniería de Estructuras, 22, 2, 113-134.

Echegaray-Aveiga, R.C., Rodríguez, F., Toulkeridis, T., & Echegaray-Aveiga, R.D. (2019). Effects of potential lahars of the Cotopaxi volcano on housing market prices. J. of Applied Volcanology, 9, 1-11.

Edler, D., Otto, K.H., & Toulkeridis, T. (2020). Tsunami hazards in Ecuador – Regional differences in the knowledge of Ecuadorian high-school students. Science of Tsunami Hazards, 39(2), 86-112.

Egbue, O., & Kellogg, J. (2010). Pleistocene to present North Andean "escape". Tectonophysics, 489(1-4), 248-257.

FEMA (2019). Guidelines for design of structures for vertical evacuation from tsunamis. FEMA P646. Washington, DC: FEMA. 202pp

Frankenberg, E., Sikoki, B., Sumantri, C., Suriastini, W., & Thomas, D. (2013). Education, vulnerability, and resilience after a natural disaster. Ecology and society: a journal of integrative science for resilience and sustainability, 18(2), 16.

Glass, J. B., Fornari, D. J., Hall, H. F., Cougan, A. A., Berkenbosch, H. A., Holmes, M. L.,... & De La Torre, G. (2007). Submarine volcanic morphology of the western Galápagos

based on EM300 bathymetry and MR1 side-scan sonar. Geochemistry, Geophysics, Geosystems, 8(3).

Griffin, J., Latief, H., Kongko, W., Harig, S., Horspool, N., Hanung, R., ... & Cummins, P. (2015). An evaluation of onshore digital elevation models for modeling tsunami inundation zones. Frontiers in Earth Science, 3, 32.

Gusiakov, V. K. (2005). Tsunami generation potential of different tsunamigenic regions in the Pacific. Marine Geology, 215(1-2), 3-9.

Gutscher, M.A., Malavieille, J.S.L., & Collot, J.-Y. (1999). Tectonic segmentation of the North Andean margin: impact of the Carnegie Ridge collision. Earth and Planetary Science Letters 168, 255–270.

Heidarzadeh, M., Murotani, S., Satake, K., Takagawa, T., & Saito, T. (2017). Fault size and depth extent of the Ecuador earthquake (Mw 7.8) of 16 April 2016 from teleseismic and tsunami data. Geophysical Research Letters, 44(5), 2211-2219.

Herd, D. G., Youd, T. L., Meyer, H., Arango, J. L., Person, W. J., & Mendoza, C. (1981). The great tumaco, colombia earthquake of 12 december 1979. Science, 211(4481), 441-445.

Herrera-Enríquez, G., Toulkeridis, T., Rodríguez-Rodríguez, G., & Albuja-Salazar (2020). Critical Factors of Business Adaptability during Resilience in Baños de Agua Santa, Ecuador, due to Volcanic Hazards . CIT, in press

Intergovernmental Oceanographic Commission. Fourth Edition. Tsunami Glossary (2019). Paris, UNESCO, IOC Technical Series, 85. (English, French, Spanish, Arabic, Chinese) (IOC/2008/TS/85 rev.4).

Ioualalen, M., Monfret, T., Béthoux, N., Chlieh, M., Adams, G. P., Collot, J. Y., ... & Gordillo, G. S. (2014). Tsunami mapping in the Gulf of Guayaquil, Ecuador, due to local seismicity. Marine Geophysical Research, 35(4), 361-378.

Ioualalen, M., Ratzov, G., Collot, J. Y., & Sanclemente, E. (2011). The tsunami signature on a submerged promontory: the case study of the Atacames Promontory, Ecuador. Geophysical Journal International, 184(2), 680-688.

Jaramillo Castelo, C.A., Padilla Almeida, O., Cruz D´Howitt, M., & Toulkeridis, T. (2018). Comparative determination of the probability of landslide occurrences and susceptibility in central Quito, Ecuador. 2018 5th International Conference on eDemocracy and eGovernment, ICEDEG 2018 8372318: 136-143.

Kanamori, H. & McNally, K.C. (1982). Variable rupture mode of the subduction zone along the Ecuador-Colombia coast. Bulletin of the Seismological Society of America, 72(4): 1241-1253.

Kassem, M. M., Nazri, F. M., & Farsangi, E. N. (2019). Development of seismic vulnerability index methodology for reinforced concrete buildings based on nonlinear parametric analyses. MethodsX, 6, 199-211.

Kates, R. W. (1976). Experiencing the environment as hazard. In Experiencing the environment (pp. 133-156). Springer, Boston, MA.

Keating, B. H., & McGuire, W. J. (2000). Island edifice failures and associated tsunami hazards. Pure and Applied Geophysics, 157(6-8), 899-955.

Kellogg, J. N., Vega, V., Stallings, T. C., & Aiken, C. L. (1995). Tectonic development of Panama, Costa Rica, and the Colombian Andes: constraints from global positioning system geodetic studies and gravity. Special Papers-Geological Society of America, 75-75.

Lukkunaprasit, P., & Ruangrassamee, A. (2008). Building damage in Thailand in the 2004 Indian Ocean tsunami and clues for tsunami-resistant design. The IES Journal Part A: Civil & Structural Engineering, 1(1), 17-30.

Lynett, P., Weiss, R., Renteria, W., Morales, G. D. L. T., Son, S., Arcos, M. E. M., & MacInnes, B. T. (2013). Coastal impacts of the March 11th Tohoku, Japan tsunami in the Galapagos Islands. Pure and Applied Geophysics, 170(6-8), 1189-1206.

Martinez, N. & Toulkeridis, T. (2020). Tsunamis in Panama – History, preparation and future consequences. Science of Tsunami Hazards, 39(2), 53-68.

Matheus Medina, A.S., Cruz D´Howitt, M., Padilla Almeida, O., Toulkeridis, T., & Haro, A.G. (2016). Enhanced vertical evacuation applications with geomatic tools for tsunamis in Salinas, Ecuador. Science of Tsunami Hazards, 35, (3): 189-213

Matheus-Medina, A.S., Toulkeridis, T., Padilla-Almeida, O., Cruz-D´ Howitt, M., & Chunga, K. (2018). Evaluation of the tsunami vulnerability in the coastal Ecuadorian tourist centers of the peninsulas of Bahia de Caráquez and Salinas. Science of Tsunami Hazards, 38(3): 175-209.

Mato, F. & Toulkeridis, T. (2017). The missing Link in El Niño's phenomenon generation. Science of tsunami hazards, 36: 128-144.

McGuire, W. J. (2006). Lateral collapse and tsunamigenic potential of marine volcanoes. Geological Society, London, Special Publications, 269(1), 121-140.

Mendoza, C., & Dewey, J. W. (1984). Seismicity associated with the great Colombia-Ecuador earthquakes of 1942, 1958, and 1979: Implications for barrier models of earthquake rupture. Bulletin of the seismological society of America, 74(2), 577-593.

Meyyappan, P., Sekar, T., & Sivapragasam, C. (2013). Investigation on Behaviour Aspects of Tsunami Resistant Structures-An Experimental Study. Disaster advances, 6(2), 39-47.

Mikami, T., Shibayama, T., Esteban, M., & Matsumaru, R. (2012). Field survey of the 2011 Tohoku earthquake and tsunami in Miyagi and Fukushima prefectures. Coastal Engineering Journal, 54(1), 1250011-1.

Moberly, R., Shepherd, G. L., & Coulbourn, W. T. (1982). Forearc and other basins, continental margin of northern and southern Peru and adjacent Ecuador and Chile. Geological Society, London, Special Publications, 10(1), 171-189.

Morales, E., Filiatrault, A., & Aref, A. (2018). Seismic floor isolation using recycled tires for essential buildings in developing countries. Bulletin of Earthquake Engineering, 16(12), 6299-6333.

Mostafizi, A., Wang, H., Cox, D., & Dong, S. (2019). An agent-based vertical evacuation model for a near-field tsunami: Choice behavior, logical shelter locations, and life safety. International journal of disaster risk reduction, 34, 467-479.

Navas, L., Caiza, P., & Toulkeridis, T. (2018). An evaluated comparison between the molecule and steel framing construction systems – Implications for the seismic vulnerable Ecuador. Malaysian Construct. Res. J. 26 (3), 87–109.

NEC (Norma Ecuatoriana de la Construcción) (2015). Estructura de Acero, Cargas No Sísmicas.

Norio, O., Ye, T., Kajitani, Y., Shi, P., & Tatano, H. (2011). The 2011 eastern Japan great earthquake disaster: Overview and comments. International Journal of Disaster Risk Science, 2(1), 34-42.

Padrón, E., Hernández, P.A., Marrero, R., Melián, G, Toulkeridis, T., Pérez., N.M., Virgili, G., & Notsu, K. (2008). Diffuse CO_2 emission rate from the lake-filled Cuicocha and Pululagua calderas, Ecuador. Journal of Volcanology and Geothermal Research (Special Volume on Continental Ecuador volcanoes), 176: 163-169.

Padrón, E., Hernández, P.A., Pérez, N.M., Toulkeridis, T., Melián, G., Barrancos, J., Virgili, G., Sumino H., & Notsu, K. (2012). Fumarole/plume and diffuse CO_2 emission from Sierra Negra volcano, Galapagos archipelago. Bull. Of Volcanol., 74: 1509-1519.

Palacios Orejuela, I. & Toulkeridis, T. (2020). Evaluation of the susceptibility to landslides through diffuse logic and analytical hierarchy process (AHP) between Macas and Riobamba in Central Ecuador. 2020 7th International Conference on eDemocracy and eGovernment, ICEDEG 2020, 200-206

Papathoma, M., & Dominey-Howes, D. (2003). Tsunami vulnerability assessment and its implications for coastal hazard analysis and disaster management planning, Gulf of Corinth, Greece. Natural Hazards and Earth System Sciences, 3(6), 733-747.

Papathoma, M., Dominey-Howes, D., Zong, Y., & Smith, D. (2003). Assessing tsunami vulnerability, an example from Herakleio, Crete. Natural Hazards and Earth System Sciences, 3(5), 377-389.

Pararas-Carayannis, G. (1977). Catalog of tsunamis in Hawaii (Vol. 4). World Data Center A for Solid Earth Geophysics.

Pararas-Carayannis, G. (1980). Earthquake and tsunami of 12 December 1979 in Colombia. Tsunami Newsletter, 13(1), 1-9.

Pararas-Carayannis, G. (2002). Evaluation of the threat of mega tsunami generation from postulated massive slope failures of island stratovolcanoes on La Palma, Canary Islands, and on the island of Hawaii. Science of Tsunami Hazards, 20(5), 251-277.

Pararas-Carayannis, G. (2003). Near and far-field effects of tsunamis generated by the paroxysmal eruptions, explosions, caldera collapses and massive slope failures of the Krakatau volcano in Indonesia on august 26-27, 1883. Science of Tsunami Hazards.

Pararas-Carayannis, G. (2006). The potential of tsunami generation along the Makran Subduction Zone in the northern Arabian Sea: Case study: The earthquake and tsunami of November 28, 1945. Science of Tsunami Hazards, 24(5), 358-384.

Pararas-Carayannis, G. (2010). The earthquake and tsunami of 27 February 2010 in Chile–Evaluation of source mechanism and of near and far-field tsunami effects. Science of Tsunami Hazards, 29, 2: 96-126.

Pararas-Carayannis, G. (2011). Tsunamigenic source mechanism and efficiency of the march 11, 2011 Sanriku earthquake in Japan. Science of Tsunami Hazards, 30(2): 126-152

Pararas-Carayannis, G. (2012). Potential of tsunami generation along the Colombia/Ecuador subduction margin and the Dolores-Guayaquil Mega-Thrust. Science of Tsunami Hazards, 31, 3: 209-230.

Pararas-Carayannis, G., & Zoll, P. (2017). Incipient evaluation of temporal El Nino and other climatic anomalies in triggering earthquakes and tsunamis - Case Study: The Earthquake and Tsunami of 16 April 2016 in Ecuador. Science of Tsunami Hazards, 36(4), 262-291.

Park, S., Van de Lindt, J. W., Gupta, R., & Cox, D. (2012). Method to determine the locations of tsunami vertical evacuation shelters. Natural hazards, 63(2), 891-908.

Pheng, L. S., Raphael, B., & Kit, W. K. (2006). Tsunamis: some pre-emptive disaster planning and management issues for consideration by the construction industry. Structural survey, 24(5), 378-396.

Pinter, N., & Ishman, S. E. (2008). Impacts, mega-tsunami, and other extraordinary claims. GSA today, 18(1), 37-38.

Poma, P., Usca, M., Fdz-Polanco, M, Garcia-Villacres, A., & Toulkeridis, T. (2020). Landslide and environmental risk from oil spill due to the rupture of SOTE and OCP pipelines, San Rafael Falls, Amazon Basin, Ecuador. CIT, in press

Pontoise, B., & Monfret, T. (2004). Shallow seismogenic zone detected from an offshore-onshore temporary seismic network in the Esmeraldas area (northern Ecuador). Geochemistry, Geophysics, Geosystems, 5(2).

Ratzov, G., Collot, J. Y., Sosson, M., & Migeon, S. (2010). Mass-transport deposits in the northern Ecuador subduction trench: Result of frontal erosion over multiple seismic cycles. Earth and Planetary Science Letters, 296(1-2), 89-102.

Ratzov, G., Sosson, M., Collot, J. Y., Migeon, S., Michaud, F., Lopez, E., & Le Gonidec, Y. (2007). Submarine landslides along the North Ecuador–South Colombia convergent margin: possible tectonic control. In Submarine mass movements and their consequences (pp. 47-55). Springer, Dordrecht.

Rentería, W., Lynett, P., Weiss, R. & De La Torre, G. (2012). Informe de la investigación de campo de los efectos del tsunami de Japón Marzo 2011, en las islas Galápagos. Acta Oceanográ ca del Pací co. Vol. 17(1): 177 - 203.

Ridolfi, F., Puerini, M., Renzulli, A., Menna, M., & Toulkeridis, T. (2008). The magmatic feeding system of El Reventador volcano (Sub-Andean zone, Ecuador) constrained by mineralogy, textures and geothermobarometry of the 2002 erupted products. Journal of Volcanology and Geothermal Research (Special Volume on Continental Ecuador volcanoes), 176: 94-106.

Robayo N, A., Llorca, J., & Toulkeridis, T. (2020). Population, territorial and economic analysis of a potential volcanic disaster in the city of Latacunga, Central Ecuador based on GIS techniques – Implications and potential solutions. In Conference on Information and Communication Technologies of Ecuador (pp. 549-563). Springer, Cham.

Rodríguez Espinosa, F., Toulkeridis, T., Salazar Martinez, R., Cueva Girón, J., Taipe Quispe, A., Bernaza Quiñonez, L., Padilla Almeida, O., Mato, F., Cruz D´Howitt, M., Parra, H., Sandoval, W., & Rentería, W. (2017). Economic evaluation of recovering a natural protection with concurrent relocation of the threatened public of tsunami hazards in central coastal Ecuador. Science of tsunami hazards, 36: 293-306.

Rodriguez, F., Cruz D´Howitt, M., Toulkeridis, T., Salazar, R., Ramos Romero, G.E., Recalde Moya, V.A., & Padilla, O. (2016). The economic evaluation and significance of an early relocation versus complete destruction by a potential tsunami of a coastal city in Ecuador. Science of tsunami hazards, 35, 1: 18-35.

Rodriguez, F., Toulkeridis, T., Padilla, O., & Mato, F. (2017). Economic risk assessment of Cotopaxi volcano Ecuador in case of a future lahar emplacement. Natural Hazards, 85, (1): 605-618.

Rodríguez, M.E. (2019). Interpretación de los daños y colapsos en edificaciones observados en la ciudad de México en el terremoto del 19 de septiembre 2017. Revista de Ingeniería Sísmica, 101, 1-18

Saji, G. (2014). Safety goals for seismic and tsunami risks: Lessons learned from the Fukushima Daiichi disaster. Nuclear Engineering and Design, 280, 449-463.

Simons, M., Minson, S.E., Sladen, A., Ortega, F., Jiang, J., Owen, S.E., Meng, L., Ampuero, J.P., Wei, S., Chu, R., & Helmberger, D.V. (2011). The 2011 magnitude 9.0 Tohoku-Oki earthquake: Mosaicking the megathrust from seconds to centuries. science, 332(6036), pp.1421-1425.

Stainforth, R. M. (1948). Applied micropaleontology in Coastal Ecuador, Jour. Paleontology, 22: 142- 146.

Suango Sánchez, V. d. R., Acosta Tafur, J.R., Rodríguez De la Vera, K., Andrade Sánchez, M.S., López Alulema, A.C., Avilés Ponce, L.R., Proaño Morales, J.L., Zambrano Benavides, M.J., Reyes Pozo, M.D., Yépez Campoverde, J.A., & Toulkeridis, T. (2019). Use of geotechnologies and multicriteria evaluation in land use policy – the case of the urban area expansion of the city of Babahoyo, Ecuador. 2019 6th International Conference on eDemocracy and eGovernment, ICEDEG 2019, 194-202.

Sun, C., Xu, J., Jia, L., Qin, Y., Zhan, K., & Zhang, J. (2017, October). Passenger Flow Assignment of Evacuation Path in the Station Based on Time Reliability. In International Conference on Electrical and Information Technologies for Rail Transportation (pp. 301-310). Springer, Singapore.

Thompson, P. A., & Marchant, E. W. (1995). A computer model for the evacuation of large building populations. Fire safety journal, 24(2), 131-148.

Titov, V. V., Moore, C. W., Greenslade, D. J. M., Pattiaratchi, C., Badal, R., Synolakis, C. E., & Kânoğlu, U. T. (2011). A new tool for inundation modeling: Community Modeling Interface for Tsunamis (ComMIT). Pure and Applied Geophysics, 168(11), 2121-2131.

Titov, V., Kânoğlu, U. and Synolakis, C. (2016). "Development of MOST for Real-Time Tsunami Forecasting." Journal of Waterway, Port, Coastal, and Ocean Engineering 142, no. 6: 03116004.

Toulkeridis, T. & Zach, I. (2017). Wind directions of volcanic ash-charged clouds in Ecuador – Implications for the public and flight safety. Geomatics, Natural Hazards and Risks, 8(2): 242-256.

Toulkeridis, T. (2011). Volcanic Galápagos Volcánico. Ediecuatorial, Quito, Ecuador: 364 pp

Toulkeridis, T. (2013). Volcanes activos Ecuador. Santa Rita, Quito, Ecuador: 152pp

Toulkeridis, T. (2016). Unexpected results of a seismic hazard evaluation applied to a modern hydroelectric plant in central Ecuador. Journal of Structural Engineering, 43, (4): 373-380.

Toulkeridis, T., Arroyo, C.R., Cruz D'Howitt, M., Debut, A., Vaca, A.V., Cumbal, L., Mato, F., & Aguilera, E. (2015a). Evaluation of the initial stage of the reactivated Cotopaxi volcano - Analysis of the first ejected fine-grained material. Natural Hazards and Earth System Sciences, 3, (11): 6947-6976.

Toulkeridis, T., Buchwaldt, R., & Addison, A. (2007). When Volcanoes Threaten, Scientists Warn. Geotimes, 52: 36-39.

Toulkeridis, T., Chunga, K., Rentería, W., Rodriguez, F., Mato, F., Nikolaou, S., Cruz D ´Howitt, M., Besenzon, D., Ruiz, H., Parra, H., & Vera-Grunauer, X. (2017b). The 7.8 M_w Earthquake and Tsunami of the 16th April 2016 in Ecuador - Seismic evaluation, geological field survey and economic implications. Science of tsunami hazards, 36: 197-242.

Toulkeridis, T., Mato, F., Toulkeridis-Estrella, K., Perez Salinas, J.C., Tapia, S., & Fuertes, W. (2018). Real-Time Radioactive Precursor of the April 16, 2016 Mw 7.8 Earthquake and Tsunami in Ecuador. Science of tsunami hazards, 37: 34-48.

Toulkeridis, T., Parra, H., Mato, F., Cruz D´Howitt, M., Sandoval, W., Padilla Almeida, O., Rentería, W., Rodríguez Espinosa, F., Salazar martinez, R., Cueva Girón, J., Taipe Quispe, A., & Bernaza Quiñonez, L. (2017a). Contrasting results of potential tsunami hazards in Muisne, central coast of Ecuador. Science of tsunami hazards, 36: 13-40

Toulkeridis, T., Porras, L., Tierra, A., Toulkeridis-Estrella, K., Cisneros, D., Luna, M.,Carrión, J.L., Herrera, M., Murillo, A., Perez-Salinas, J.C., Tapia, S., Fuertes, W., & Salazar, R. (2019). Two independent real-time precursors of the 7.8 Mw earthquake in Ecuador based on radioactive and geodetic processes - Powerful tools for an early warning system. Journal of Geodynamics, 126: 12-22

Toulkeridis, T., Rodríguez, F., Arias Jiménez, N., Simón Baile, D., Salazar Martínez, R., Addison, A., Freyre Carryon, D., Mato, F., & Díaz Perez, C. (2016). Causes and consequences of the sinkhole at El Trébol of Quito, Ecuador - Implications for economic damage and risk assessment. Natural Hazards and Earth Science System, 16: 2031–2041

Toulkeridis, T., Rojas-Agramonte, Y., & Noboa, G. P. (2020c). Ocean Policy of the UNCLOS in Ecuador Based on New Geodynamic and Geochronological Evidences. Smart Innovation, Systems and Technologies., 181: 485-495

Toulkeridis, T., Seqqat, R., Torres, M., Ortiz-Prado, E., & Debut, A. (2020b). COVID-19 Pandemic in Ecuador: a health disparities perspective. Revista de Salud Publica de Colombia, 22 (3), 1-5.

Toulkeridis, T., Simón Baile, D., Rodríguez, F., Salazar Martínez, R., Arias Jiménez, N., & Carreon Freyre, D. (2015b). Subsidence at the "trébol" of Quito, Ecuador: An indicator for future disasters?. Proceedings of the International Association of Hydrological Sciences, Volume 372, 12 November 2015: 151-155

Toulkeridis, T., Tamayo, E., Simón-Baile, D., Merizalde-Mora, M.J., Reyes –Yunga, D.F., Viera-Torres, M., & Heredia, M. (2020a). Climate change according to Ecuadorian academics–Perceptions versus facts. La Granja, 31(1), 21-49

Tsai, J., Fridman, N., Bowring, E., Brown, M., Epstein, S., Kaminka, G. A., ... & Tambe, M. (2011, May). ESCAPES: evacuation simulation with children, authorities, parents, emotions, and social comparison. In AAMAS (Vol. 11, pp. 457-464).

Vaca, A.V., Arroyo, C.R., Debut, A., Toulkeridis, T., Cumbal. L., Mato, F., Cruz D´Howitt, M., & Aguilera, E. (2016). Characterization of fine-grained material ejected by the cotopaxi volcano employing X-ray diffraction and electron diffraction scattering. Biology and Medicine, 8: 3

Whelan, F., & Kelletat, D. (2003). Submarine slides on volcanic islands-a source for mega-tsunamis in the Quaternary. Progress in Physical Geography, 27(2), 198-216.

Wood, N., Jones, J., Schelling, J., & Schmidtlein, M. (2014). Tsunami vertical-evacuation planning in the US Pacific Northwest as a geospatial, multi-criteria decision problem. International journal of disaster risk reduction, 9, 68-83.

Yeh, H. H. J., Robertson, I., & Preuss, J. (2005). Development of design guidelines for structures that serve as tsunami vertical evacuation sites (Vol. 4). Washington: Washington State Department of Natural Resources, Division of Geology and Earth Resources.

Yépez, V., Toledo, J., & Toulkeridis, T. (2020). The Armed Forces as a State institution in immediate response and its participation as an articulator in the risk management in Ecuador. Smart Innovation, Systems and Technologies 181, 545-554.

Zafrir Vallejo, R., Padilla-Almeida, O., Cruz D´Howitt, M., Toulkeridis, T., Rodriguez Espinosa, F., Mato, F., & Morales Muñoz, B. (2018). Numerical probability modeling of past, present and future landslide occurrences in northern Quito, Ecuador – Economic implications and risk assessments. 2018 5th International Conference on eDemocracy and eGovernment, ICEDEG 2018 8372318: 117-125.

Zapata, A.,, Sandoval, J., Zapata, J., Ordoñez, E., Suango, V., Moreno, J., Mullo, C., Tipán, E., Rodríguez, K.E., & Toulkeridis, T. (2020). Application of quality tools for evaluation of the use of geo-information in various municipalities of Ecuador. In Conference on Information and Communication Technologies of Ecuador (pp. 420-433). Springer, Cham.

Zhang, L., Liu, M., Wu, X., & AbouRizk, S. M. (2016). Simulation-based route planning for pedestrian evacuation in metro stations: A case study. Automation in Construction, 71, 430-442.

Zhong, M., Shi, C., Tu, X., Fu, T., & He, L. (2008). Study of the human evacuation simulation of metro fire safety analysis in China. Journal of Loss Prevention in the Process Industries, 21(3), 287-298.